### 67.5.2 Basal motion

Field research indicates that basal motion is essentially governed by a small number of factors, including basal shear traction, bed temperature and the presence and pressure of water at the basal interface (whether hard or soft). Basal water pressure is the least-well constrained of these controls, being governed by a balance between water delivery to the glacier base and water removal from it. Although our understanding of spatial and temporal variations in basal water pressure at temperate valley glaciers is now fairly well advanced, little is known about these variables beneath larger and/or thermally complex ice masses. There is therefore a pressing need for field programmes that simultaneously record motion components and their principal controls at these ice masses. Indeed, some work has already begun in this arena. Bingham *et al.* (2003), for example, report systematic annual and seasonal motion variations at polythermal John Evans Glacier in the Canadian Arctic.

This lumped basal motion approach should develop in tandem with further detailed investigations of specific processes of basal motion. For example, the effects of variations in bedrock roughness and the integrity of the basal drainage system are currently neglected in sliding models. The balance between sliding by slip, enhanced deformation and regelation also needs to be formalized, perhaps as functions of stress regime, location and basal temperature. Similarly, controls over processes and rates of subglacial sediment deformation need further investigation. Ultimately, a constitutive relation for subglacial sediments is required. This relation should include terms for processes such as ploughing and perhaps even terms for grain-size evolution and the development of clast fabric that models could calculate in a time-evolving manner. Finally, basal motion at subfreezing temperatures also needs to be investigated more thoroughly and at the glacier-wide scale, both at hard- and soft-bedded glaciers.

SIXTY-EIGHT

# *Measurements and modelling of diurnal flow variations in a temperate valley glacier*

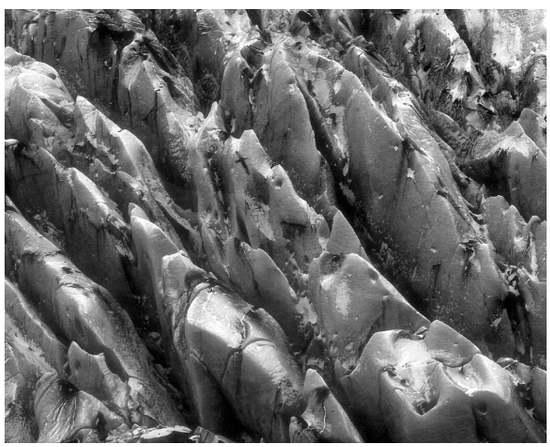

**Shin Sugiyama**

*Section of Glaciology, Versuchsanstalt für Wasserbau Hydrologie und Glaziologie, ETH, Gloriastrasse 37/39, CH-8092 Zürich, Switzerland*

## 68.1 Introduction

During the ablation season, surface melting causes diurnal flow variations in temperate glaciers. Because basal motion plays a key role in short-term velocity fluctuations, measurements of diurnal flow variations provide insight into subglacial conditions and their influence on the glacier flow field.

This contribution reports high-frequency measurements of diurnal flow speed and strain rate variations in a temperate valley glacier in the Swiss Alps. Numerical simulations of the observed flow field using a two-dimensional finite-element flow model indicated that basal motion was non-uniformly distributed along the glacier and its pattern varied in a diurnal manner.

## 68.2 Field measurements

Measurements were carried out in the ablation area of Lauteraargletscher, Switzerland (Fig. 68.1) from 22 to 27 August 2001. A 6.5-m-long aluminium pole was installed on the surface and continuously surveyed with GPS (Global Positioning System) to obtain hourly records of horizontal flow speed and vertical displacement. Three other poles were also surveyed twice a day at 0600 hours and 1800 hours to compute the horizontal surface strain rate. The precise distance (±5 mm) from the base of a ca. 173-m-long borehole to a surface reference was also measured in order to calculate the vertical strain of ice over the depth of the borehole (Gudmundsson, 2002; Sugiyama & Gudmundsson,

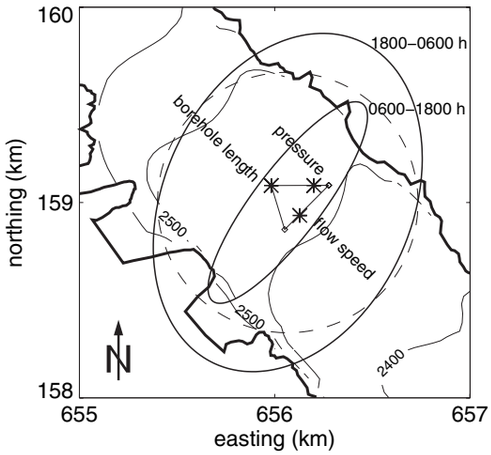


**Figure 68.1** Map of the study site on Lauteraargletscher, showing the locations of the surface and borehole measurement sites and the strain grid. The two ellipses are strain rate ellipses during the indicated time periods of the days from 22 to 27 August 2001. These ellipses represent the deformation of the circle (broken line) subjected to the computed surface strain rate in units of $10^{-4}$ day$^{-1}$.

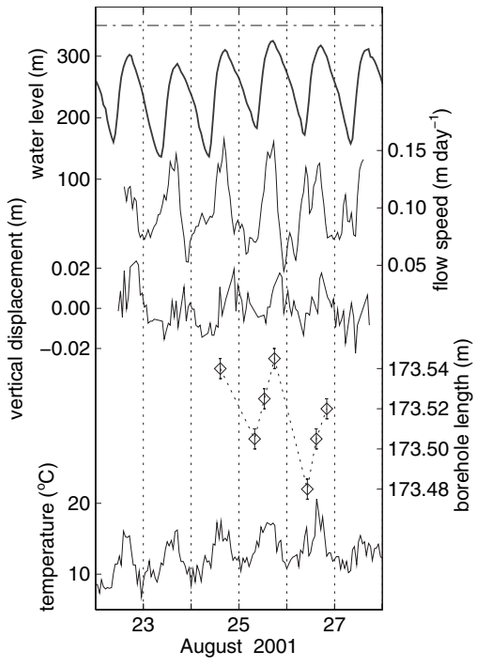


**Figure 68.2** Records of water level in a borehole, horizontal flow speed, vertical displacement of the surface relative to the mean elevation, borehole length and air temperature. The dash–dot line at the top indicates the water level corresponding to the ice overburden.

2003). A water-pressure transducer was also installed in a nearby borehole to measure the water level every 10 min.

Results of the measurements are shown together with air temperature recorded at the glacier flank, in Fig. 68.2. During the study period, 40–60 mm w.e. of daily ablation took place, and the borehole water level oscillated more than 100 m diurnally. The surface flow-speed showed clear diurnal variations, reaching a maximum in the afternoon and a minimum in the morning. Diurnal variations are also observed in the vertical displacement and the borehole length. Peaks in flow speed coincide with water-level maxima, suggesting that basal motion was enhanced by high subglacial water pressure. These peaks also coincide with the maximum rate of upward vertical displacement. Surface uplift during fast-flow events has been considered to result from the formation of water-filled basal cavities (Iken *et al.*, 1983). Nevertheless, the observed uplift cannot be attributed totally to basal cavity formation as the borehole length measurements showed vertical tensile strains at times when the surface moved upward. These vertical strain rates reached $5 \times 10^{-4}$ day$^{-1}$. The horizontal surface strain data (Fig. 68.1) indicate compression along the flow direction during the daytime (0600–1800 hours), which is consistent with the vertical extension. These changes in the strain regime indicate consistent systematic diurnal variations in the spatial pattern of flow speed along the glacier.

During the same period, we operated two further GPS receivers located 1.5 km up-glacier and down-glacier from the main study site. Although diurnal velocity variations were recorded at all three sites, those up-glacier of the main study site were greatest. This suggests that the measured vertical extension during the daytime was probably caused by a compressive flow established at the study site. Because the seasonal snow line was about 1 km up-glacier, it is plausible that the highest peak diurnal pressure was greater in the upper reach owing to less developed subglacial drainage conditions (Nienow *et al.*, 1998). The compressive flow field dissipated overnight as subglacial water drained down-glacier and flow speed slowed down.

## 68.3 Numerical modelling

To test the hypothesis proposed above, the englacial flow field was investigated with a finite-element glacier flow model. The aim of the modelling was to prescribe basal conditions to reproduce the measured diurnal variations in flow speed and vertical strain rate.

### 68.3.1 Model configuration

The model computes flow-velocity fields in a longitudinal cross-section of a slab, based on Stokes' equations and Glen's flow law with $n = 3$ (Sugiyama *et al.*, 2003). A finite-element scheme was used to solve the differential equations for two components of the flow velocity, using quadratic triangle elements with horizontal and vertical grid sizes of 500 m and 50–100 m, respectively. Basal motion was introduced in the form:

$$u_b(x) = c(x)\tau_b^{n'}$$

where $u_b(x)$ is the basal sliding speed at the longitudinal coordinate $x$, $\tau_b$ is the basal shear stress, and $n'$ and $c(x)$ are parameters

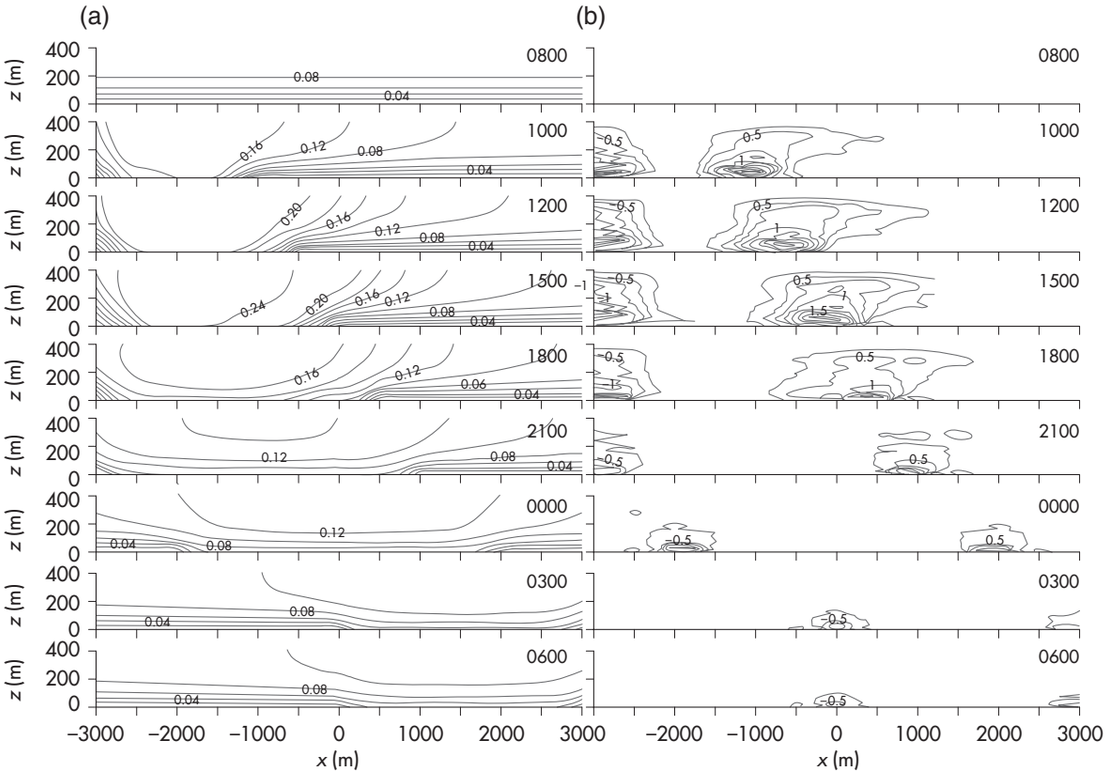


**Figure 68.3** Englacial flow fields in a longitudinal cross-section computed for the times indicated in the figures. (a) Horizontal flow speed (m day$^{-1}$). (b) Vertical strain rate ($10^{-4}$ day$^{-1}$). Positive value indicates tensile strain rate.

of the sliding law. We assume $n' = 1$, and prescribe $c(x)$ in order to reproduce the observed diurnal flow variations.

### 68.3.2 Model output

Horizontal flow speed and vertical strain rate were computed for a region between 3 km up-glacier and down-glacier of the study site (Fig. 68.3). Ice thickness at the study site was modelled to be 400 m. No sliding $c(-3000 < x < 3000) = 0$ was assumed at 0800 hours when the surface speed was at a minimum, and then $c(x)$ was determined for each time of day so that the computed surface-flow speeds at $x = 0$ agree to within 10% of the measurements on 25 August (Fig 68.3a). This 10% tolerance was within GPS measurement errors. Based on the hypothesis that the basal motion was higher in the upper reach, a sliding zone with greater value of $c$ was allocated up-glacier of the study site at 1000 hours and its magnitude increased during the daytime. The position of the sliding zone was then gradually moved down-glacier at night, reducing the magnitude of $c$ toward next morning.

Output from the model recreates the principal features of the field measurements:

1. vertical strain rate is tensile during the day from 1000 to 1800 hours;
2. magnitude of the strain rate reaches $10^{-4}$ day$^{-1}$ at 1500 hours at $x = 0$;
3. diurnal velocity variation is greater up-glacier.

Although the computed strain rate is still smaller than that measured in the borehole, the basal sliding zone established in the upper reach and its temporal evolution was able to explain the diurnal flow variations in Lauteraargletscher.

## 68.4 Discussion

High temporal resolution measurements of surface velocity and vertical strain rate indicated systematic diurnal flow variations in a temperate valley glacier. These data are consistent with a cause related to spatially and temporally non-uniform basal motion.

These surface flow fluctuations are not simply the results of variations in local basal motion, but also of variations in neighbouring basal and englacial motion, as shown in Fig. 68.3. Thus, the spatial distribution of basal motion and its transfer to the englacial flow field control short-term flow variations in temperate glaciers. High-frequency measurements of the englacial flow field are crucial to improve our understanding in this research field and accurate computation of the glacier flow field is important to infer bed conditions and basal-flow processes from surface observations.

SIXTY-NINE

# *Using field data to constrain ice-flow models: a study of a small alpine glacier*

**Alun Hubbard**

*Department of Geography, University of Edinburgh, Edinburgh EH8 9XP, UK*

This case study is concerned with the application of a three-dimensional ice flow model to Haut Glacier d'Arolla, a small temperate glacier in the Swiss Alps. The study illustrates both the potential and certain limitations of using high-resolution, three-dimensional flow modelling constrained by observations to aid our understanding of alpine glacier systems. In particular, the combination of flow modelling with detailed field measurements at Haut Glacier d'Arolla provides a powerful tool to investigate its rheological properties, the interaction between basal hydrology and ice dynamics, the occurrence and formation of surface structures, its past and present response and, ultimately, its future trajectory to climate change.

The model is based on Blatter's (1995) solution of the mass and force balance equations using a non-linear rheology (with the flow law exponent: $n = 3$) applied to the surface and bed topography of Haut Glacier d'Arolla at 70 m horizontal resolution with 40 vertical layers scaled to thickness. The model is steady-state; it computes the instantaneous stress and strain distribution based on Glen's (1958a) flow law:

$$\dot{\varepsilon}_{ij} = A\tau_e^{n-1}\tau_{ij}$$

where $\dot{\varepsilon}_{ij}$ is the strain rate tensor, $A$ is the rate factor reflecting ice hardness, $\tau_{ij}$ is the imposed stress tensor and $\tau_e$ is the effective stress given by

$$2\tau_e^2 = 2(\tau_{xz}^2 + \tau_{xy}^2 + \tau_{yz}^2) + \tau'^2_{xx} + \tau'^2_{yy} + \tau'^2_{zz}$$

The model computes first-order terms, that is longitudinal and transverse deviatoric stresses ($\tau'_{xx}$ and $\tau'_{yy}$) which result in compression and tension throughout the ice mass and which, in extreme circumstances, lead to observed structural failure such as overthrusting, shearing and crevassing. The resulting solution is highly dependent on the basal boundary condition, which can be specified as either a velocity or drag distribution or a combination of both, which enables the spatial interaction of slip/stick patchiness resulting from heterogeneity in the bulk subglacial properties, such as roughness, hydrology, effective pressure and sediment strength, to be modelled. This is achieved through the prescription of zero or reduced basal shear traction to replicate decoupled, low drag zones, whereas zero velocity or increased shear traction can be prescribed to simulate 'sticky' zones. For the purposes of initial model optimization though, the model is first specified with zero sliding across the whole of the bed.

By holding the flow-law exponent ($n$) constant then the only parameter that requires 'tuning' is the rate factor ($A$) related to ice viscosity. Assuming Haut Glacier d'Arolla to be temperate with negligible basal motion during winter, then comparison of modelled with observed winter surface velocities provides an effective means for calibrating $A$. Observations that winter surface velocities are consistently low and, furthermore, that there is virtually no supraglacial melt-water available to drive ice–bed separation, lend tentative support for this assumption. Tuning of the model against surface velocities measured over 10 days in January 1995 yields an optimum value of $A = 0.063\,\mathrm{yr}^{-1}\,\mathrm{bar}^{-3}$, corresponding to an $R^2 = 0.74$ on a bivariate plot of modelled against measured surface velocities (Fig. 69.1). Although this value is half that expected (Paterson, 1994) it does lie within a narrow range of $0.07 \pm 0.01\,\mathrm{yr}^{-1}\,\mathrm{bar}^{-3}$ reported for other temperate glaciers modelled using higher order solutions (e.g. Gudmundsson, 1999). Such consistency lends confidence in the predictive quality of the internal strain component of these models but also suggests that they may be applied to temperate ice masses without significant tinkering with the rate factor.

Computation of the full stress and strain field enables model comparison with additional observables such as the occurrence and orientation of crevassing and measured principal strains. Comparison of zones of maximum computed surface tensile strain and their direction with the actual distribution and orientation of crevassing reveals a good general correspondence (Fig. 69.2a & b). Furthermore, the orientation of modelled principal strain faithfully reproduces the pattern measured from repeat survey of a dense network of strain diamonds from 1994 to 1995 (Fig. 69.3a & b). However, it is apparent that even though their